Çukurova Üniversitesi
Mühendislik Fakültesi Dergisi
Çukurova University
Journal of the Faculty of Engineering
ISSN: 2757-9255 CİLT/VOLUME: 41 SAYI/ISSUE: 2 HAZİRAN/JUNE 2026

A Novel Energy-Efficient Optimization Framework for AVR Controllers in Modern Power Systems

Ömer TÜRKSOY [1,a]

[1]*İskenderun Technical University, Faculty of Engineering and Natural Sciences, Department of Electrical-Electronic Engineering, İskenderun/Hatay, Türkiye*

[a]***ORCID***: *0000-0003-4620-4503*

Article Info
Received : 07.11.2025
Accepted : 06.01.2026
DOI: 10.21605/cukurovaumfd.1895845

Corresponding Author
Ömer TÜRKSOY
omer.turksoy@iste.edu.tr

Keywords
Automatic voltage regulator
Controller optimization
Energy-efficient objective function
Particle swarm optimization
Sustainable power systems

How to cite: *TÜRKSOY, Ö., (2026). Numerical Investigation of Channel Configuration on Thermal Behavior of Liquid-Cooled Plates in Cylindrical Lithium-Ion Battery Modules. Cukurova University, Journal of the Faculty of Engineering, 41(2), 399-416.*

ABSTRACT

Energy efficiency has become a critical objective in modern power system control due to sustainability requirements and the increasing penetration of renewable energy sources. This paper proposes a novel energy-efficient optimization framework for AVR systems to ensure reliable voltage regulation while minimizing control energy. The framework is based on a newly defined EEPI, integrating voltage tracking accuracy and control-signal energy into a unified objective function. Unlike conventional indices prioritizing fast transient response, the EEPI enables a systematic trade-off between dynamic performance and energy consumption, selecting a Pareto-balanced operating point. The approach is applied to PID and FOPID controllers optimized using the PSO algorithm. Practical feasibility is verified through Processor-in-the-Loop implementation on a TMS320F28035 platform. Comparative results with IAE, ISE, ITAE, ITSE, ZLG, and TR indices show that EEPI reduces control energy while preserving acceptable transient performance, providing a scalable solution for sustainable AVR controller design.

Modern Güç Sistemlerinde AVR Kontrolörleri için Yeni Bir Enerji Verimli Optimizasyon Çerçevesi

Makale Bilgileri
Geliş : 07.11.2025
Kabul : 06.01.2026
DOI: 10.21605/cukurovaumfd.1895845

Sorumlu Yazar
Ömer TÜRKSOY
omer.turksoy@iste.edu.tr

Anahtar Kelimeler
Enerji verimli amaç fonksiyonu
Kontrolör optimizasyonu
Otomatik gerilim regülatörü
Parçacık sürü optimizasyonu
Sürdürülebilir güç sistemleri

Atıf şekli: *TÜRKSOY, Ö., (2026). Modern Güç Sistemlerinde AVR Kontrolörleri için Yeni Bir Enerji Verimli Optimizasyon Çerçevesi. Çukurova Üniversitesi, Mühendislik Fakültesi Dergisi, 41(2), 399-416.*

ÖZ

Enerji verimliliği, sürdürülebilirlik gereksinimleri ve yenilenebilir enerji kaynaklarının artan entegrasyonu nedeniyle modern güç sistemi kontrolünde kritik bir tasarım hedefi haline gelmiştir. Bu çalışmada, güvenilir gerilim regülasyonu sağlarken kontrol enerjisini en aza indirmeyi amaçlayan, Otomatik Gerilim Regülatörü sistemleri için yeni bir enerji verimli optimizasyon çerçevesi önerilmektedir. Önerilen çerçeve, gerilim izleme doğruluğu ile kontrol sinyali enerjisini tek bir amaç fonksiyonunda birleştiren yeni tanımlanmış EEPI üzerine kuruludur. Hızlı geçici rejimi önceliklendiren geleneksel performans indekslerinin aksine, EEPI dinamik performans ile enerji tüketimi arasında sistematik bir denge kurarak Pareto-dengeli bir çalışma noktası seçmektedir. Yöntem, PSO algoritması ile optimize edilen PID ve FOPID kontrolörlerine uygulanmıştır. Pratik uygulanabilirlik, TMS320F28035 platformunda PIL gerçekleştirmesi ile doğrulanmıştır. IAE, ISE, ITAE, ITSE, ZLG ve TR indeksleri ile yapılan karşılaştırmalar, EEPI'nin kabul edilebilir geçici rejim performansını korurken kontrol enerjisini azalttığını göstermektedir. Bu sonuçlar, sürdürülebilir AVR kontrolör tasarımı için ölçeklenebilir bir çözüm sunmaktadır.

1. INTRODUCTION

In modern electrical power systems, the reliable transfer of generated power to consumers is crucial for both economic and technical reasons. During this process, load variations, demand fluctuations, and the growing penetration of renewable energy resources frequently lead to deviations in voltage magnitude and frequency. Such deviations directly affect the performance and lifespan of electrical devices, reduce overall system efficiency, and in severe cases may result in instability or outages. Therefore, maintaining voltage quality and system stability remains a fundamental challenge for power engineers [1-3].

The AVR system is widely recognized as one of the most effective mechanisms for maintaining terminal voltage stability in synchronous generators. By dynamically adjusting the excitation voltage, the AVR preserves the reactive power balance of the power system and ensures proper operation under varying conditions [4]. However, the performance of an AVR system is highly dependent on the design and tuning of its controller. Among conventional approaches, the PID controller has been extensively employed due to its simplicity, reliability, and ease of implementation [5]. Subsequently, the FOPID controller was introduced to enhance tuning flexibility by incorporating fractional integration and differentiation parameters [6]. Although a variety of fast and robust control strategies have been proposed in the literature, PID and FOPID remain the most practical and widely preferred solutions for AVR applications, as they provide a favorable balance between effectiveness and implementation simplicity. Nevertheless, improper tuning of these controllers may still result in degraded transient behavior or poor steady-state performance [7].

To address this challenge, a wide variety of optimization algorithms have been employed for AVR controller tuning, ranging from classical techniques to modern metaheuristic approaches such as PSO [8], GA [9], DE [10], ABC [10], GWO [11], CSA [12], and many others. These algorithms are designed to efficiently explore large and complex parameter spaces where traditional analytical methods are insufficient. The performance of the selected optimization algorithm directly affects the overall quality of the AVR system response. Algorithms that fail to escape local optima may yield poorly tuned controller parameters, leading to unsatisfactory transient or steady-state behavior. Hence, robust and globally convergent optimization strategies are essential to ensure reliable AVR performance [13].

Beyond the optimization algorithm itself, the formulation of the objective function plays a decisive role in determining system performance [14]. Even highly advanced algorithms cannot deliver reliable results if the objective function fails to accurately capture the inherent trade-offs among key performance metrics. In AVR control design, improving one performance aspect often comes at the expense of another; for instance, aggressive tuning may reduce rise time but increase control effort and energy consumption. Therefore, the controller tuning problem can be naturally interpreted as a multi-objective optimization task, where dynamic response and control energy form competing objectives. From this perspective, the goal is not to maximize a single metric, but to achieve a balanced operating point within the Pareto-optimal trade-off surface.

Traditionally, performance indices such as IAE, ISE, ITAE, and ITSE have been widely used for AVR tuning [15-17]. These indices provide meaningful insights into transient characteristics, including rising time, settling time, overshoot, and steady-state error. In recent years, modified and hybrid objective functions have been proposed to overcome the limitations of classical indices. Among these, the ZLG objective function [8] has gained prominence due to its ability to penalize overshoot and improve settling performance, leading to well-balanced transient responses. Similarly, alternative indices such as the TR objective function [18] have been introduced to enhance robustness under parameter uncertainties and disturbances. However, a common limitation of these approaches is that they predominantly emphasize dynamic performance metrics while neglecting control effort and associated energy consumption. With the rapid integration of renewable energy sources, distributed generation, and electric vehicles, the efficiency of control actions has become increasingly important, since excessive and high-amplitude control signals lead to unnecessary energy usage and reduced sustainability. In addition to energy consumption, highly oscillatory control signals introduce excessive switching stress on power electronic and control hardware components, which accelerates thermal degradation and reduces the operational lifetime of switching devices. Over extended operation, this effect may significantly increase maintenance and replacement costs, highlighting the practical importance of minimizing unnecessary control activity alongside energy usage.

Table 1 presents a survey of representative AVR controller studies and the objective functions employed in their optimization frameworks. While these approaches have advanced the field considerably, a notable research gap persists; none of the existing performance indices explicitly integrate control energy as a primary design criterion. In most previous studies, energy consumption has been treated as a secondary or implicit consequence rather than a core objective of the optimization process. This limitation becomes particularly significant in modern power systems, where energy-aware operation and sustainability are key design priorities.

Motivated by this gap, the present study proposes a novel energy-efficient optimization framework for AVR controllers based on a newly developed EEPI. Unlike conventional indices, the EEPI directly accounts for the energy of the control signal and explicitly incorporates the trade-off between transient response and energy consumption. From a multi-objective standpoint, the proposed formulation identifies a Pareto-balanced solution rather than prioritizing aggressive transient speed. The proposed framework is applied to PID and FOPID controllers, with optimal parameters obtained using the PSO algorithm. The performance of the EEPI is systematically compared with four widely used classical indices (IAE, ISE, ITAE, ITSE), the established hybrid ZLG function, and the recently introduced TR index. Simulation and PIL–based results demonstrate that the proposed approach achieves significant reductions in control energy while maintaining acceptable dynamic performance. These findings highlight energy-aware optimization as a promising direction for developing sustainable AVR control strategies in modern power systems.

Table 1. Summary of representative AVR controller studies and objective functions

Ref#	Year	Type of controller	Optimization algorithm	Objective function
Proposed	2026	PID, FOPID	PSO	EEPI
[18]	2025	PIDF + Fuzzy PIDF	TLBO	ITAE
[19]	2025	PID	ADIWACO PSO	ITAE
[20]	2025	FFOPIDF	TLBO	ZLG
[21]	2025	RPIDD^2 -PI	ECSA	ZLG
[22]	2024	3-DOF-PIDA	SSO	ITSE
[23]	2024	PIDD^2	HWO	ITAE
[24]	2024	SMC	GWO, SCA	TR
[25]	2024	PIDD^2	HH+SA	ZLG
[26]	2024	FOPID+ D^2	MGO	ZLG
[27]	2024	FOPID-LP	hPSO	ITAE, CTDOF
[28]	2024	1DOF-PID	hVsaGwo	ISE
[13]	2024	SFOPID	DO	ISE, IAE, ITSE, ITAE, ZLG
[29]	2022	SMC	PSO	CTDOF
[30]	2021	PID	MRFO	ZLG
[31]	2021	PID	EO	ZLG
[32]	2021	2DOF-PI	PSO, VSA, SCA, GWO, SSA, MFO, WCA	ITSE
[33]	2020	PID	TSA	ZLG
[34]	2020	FOPID	JOA	ITAE
[35]	2019	PID	IKA	ITSE+ZLG
[36]	2019	PID	WWO	ITAE
[37]	2018	PID	SFS	ITSE
[5]	2016	PID	TLBO	ZLG

2. AVR SYSTEM AND CONTROLLERS

2.1. AVR System Model with Limiters

The AVR is a critical component in synchronous generator systems, regulating excitation voltage to maintain the terminal voltage within desired operational limits. By performing this function, the AVR contributes to preserving reactive power balance, improving voltage stability, and enhancing the overall reliability of the power system under varying loading conditions.

The AVR structure is composed of four main functional subsystems: amplifier, exciter, synchronous generator, and sensor. These elements operate in a coordinated manner to adjust the excitation signal in response to deviations in terminal voltage. A schematic representation of the system structure is illustrated in Figure 1.

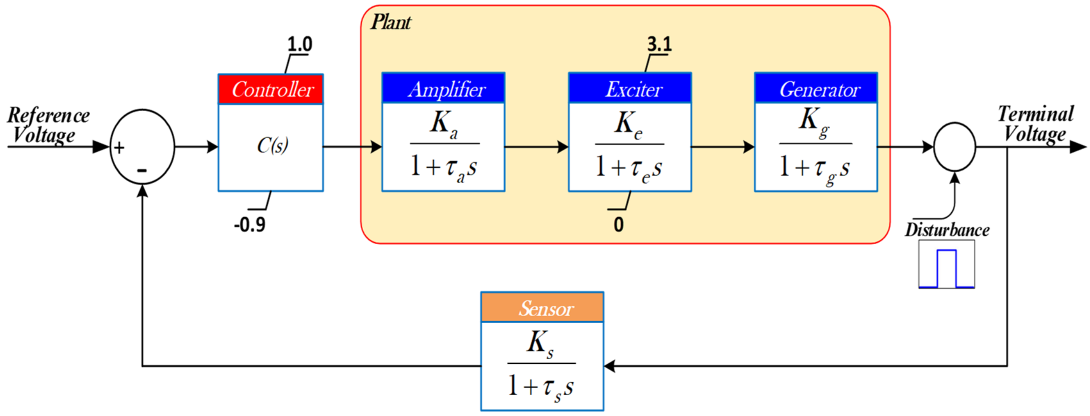

Figure 1. A schematic representation of the system structure

Each subsystem is modeled using a linearized first-order transfer function to represent its dynamic behavior. This modeling approach provides a simplified yet effective representation of the dominant dynamics of voltage regulation, making it suitable for controller design and performance evaluation.

The gain and time constant parameters of each block are selected within practical operating ranges, as summarized in Table 2 are adopted from standard AVR models reported in the literature [24,25].

Table 2. The gain and time constant parameters

Component	Transfer function	Range of the gain	Range of the time constant(s)	Chosen values
Amplifier	$G_a(s) = \frac{K_a}{(1+\tau_a s)}$	$10 \le K_a \le 40$	$0.02 \le \tau_a \le 0.1$	$K_a = 10$, $\tau_a = 0.1$
Exciter	$G_e(s) = \frac{K_e}{(1+\tau_e s)}$	$1 \le K_e \le 10$	$0.1 \le \tau_e \le 0.4$	$K_e = 1.0$, $\tau_e = 0.4$
Generator	$G_g(s) = \frac{K_g}{(1+\tau_g s)}$	$0.7 \le K_g \le 1.0$	$1.0 \le \tau_g \le 2.0$	$K_g = 10$, $\tau_g = 0.1$
Sensor	$G_s(s) = \frac{K_s}{(1+\tau_s s)}$	$0.9 \le K_s \le 1.1$	$0.001 \le \tau_s \le 0.06$	$K_s = 10$, $\tau_s = 0.1$

The overall AVR transfer function can be expressed as:

$$G_{AVR}(s) = \frac{K_A}{1+\tau_A s} \cdot \frac{K_E}{1+\tau_E s} \cdot \frac{K_G}{1+\tau_G s} \cdot \frac{K_S}{1+\tau_S s} \tag{1}$$

where K_A, K_E, K_G and K_S denote the gains, and τ_A, τ_E, τ_G and τ_S represent the time constants associated with the amplifier, exciter, generator, and sensor subsystems, respectively.

Although this linearized representation simplifies system analysis, real AVR systems exhibit nonlinear characteristics, particularly due to actuator limits and saturation effects. To enhance modeling realism, limiter mechanisms are introduced in both the controller and exciter blocks. The exciter limiter constrains the excitation signal to prevent excessive under- or over-excitation, while the controller limiter ensures that the control signal remains within physically feasible voltage bounds. These nonlinearities significantly influence transient response characteristics and reflect practical implementation constraints [38].

In this work, an excitation system configuration analogous to the DC1C [24,29,39] structure is adopted, incorporating saturation behavior and bounded control signal constraints. The DC1C excitation model represents a conventional IEEE Type-1 DC excitation system widely used in synchronous generator voltage regulation studies, characterized by first-order exciter dynamics, saturation effects, and practical excitation limits. In order to reflect realistic operating conditions, the exciter output is constrained within a physically feasible range, where the excitation voltage is limited between 0 and 3.1 p.u. This saturation bound prevents excessive over-excitation and ensures stable operation of the excitation system under large disturbances. Incorporating these nonlinear constraints improves the physical consistency of the model and enables more realistic evaluation of controller performance under practical operating conditions.

2.2. PID Controller

The PID controller is one of the most widely utilized control structures in AVR applications due to its simple structure, ease of implementation, and satisfactory performance in practical power systems. Despite the emergence of advanced control strategies, PID controllers remain a preferred choice in voltage regulation tasks because they provide an effective compromise between control performance and computational complexity.

The control law of the PID controller is formulated based on the instantaneous error signal, its accumulated integral, and its rate of change. Accordingly, the transfer function of the PID controller can be expressed as:

$$G_{PID}(s) = K_p + \frac{K_i}{s} + K_d s \tag{2}$$

where K_p, K_i, and K_d represent the proportional, integral, and derivative gains, respectively.

The proportional term primarily determines the system's response speed, the integral term ensures elimination of steady-state error, and the derivative term contributes to improving damping and transient stability. However, the dynamic behavior of the AVR system is highly sensitive to the selection of these parameters. Improper tuning may cause excessive overshoot, long settling times, oscillatory response, or even instability.

For this reason, the PID controller parameters cannot be selected using heuristic or trial-and-error approaches, especially in systems where performance and efficiency are critical. Instead, systematic optimization-based tuning methods are required to achieve a balanced trade-off between fast voltage recovery, low overshoot, and stable steady-state operation. In this study, the PID controller parameters are optimized using a structured optimization framework, aiming not only to improve transient response but also to minimize unnecessary control energy through the proposed EEPI.

This formulation allows the PID controller to operate in an energy-aware manner, ensuring that high performance is achieved without excessive control effort, which directly supports the objective of sustainable and efficient voltage regulation.

2.3. FOPID Controller

The FOPID controller extends the classical PID structure by introducing fractional orders in the integral and derivative terms. This extension provides additional flexibility in controller design, enabling more precise shaping of the system dynamics and improved robustness against parameter uncertainties and external disturbances.

The transfer function of the FOPID controller is given by:

$$G_{FOPID}(s) = K_p + \frac{K_i}{s^{\lambda}} + K_d s^{\mu} \tag{3}$$

where K_p, K_i, and K_d denote the controller gains, and λ and μ represent the fractional orders of integration and differentiation, respectively, with $0<\lambda,\mu\leq 1$.

Compared to conventional PID controllers, the FOPID structure provides enhanced control flexibility by allowing independent adjustment of the memory and dynamic behavior of the system. This makes it particularly suitable for systems exhibiting complex dynamics such as AVR plants with nonlinearities and saturation effects. However, the increased number of tuning parameters introduces a higher-dimensional optimization problem, requiring an effective, well-designed optimization strategy.

In this study, the FOPID controller is incorporated to evaluate the generality and scalability of the proposed energy-efficient optimization framework. By comparing the performance of PID and FOPID controllers under the same EEPI-based tuning scheme, the capability of the proposed method to handle both classical and advanced controller structures is systematically assessed.

3. OBJECTIVE FUNCTIONS IN AVR CONTROLLER OPTIMIZATION

The performance of an Automatic Voltage Regulator system is strongly influenced by the selection of the objective function used during controller parameter optimization. While the optimization algorithm determines how efficiently the search space is explored, the objective function defines what constitutes optimal behavior. Consequently, the effectiveness of any optimization-based tuning framework depends primarily on the ability of the objective function to accurately reflect the desired control objectives.

In AVR controller design, objective functions are typically formulated based on time-domain error signals, aiming to improve transient response characteristics such as rising time, settling time, overshoot, and steady-state error. Over the years, a variety of performance indices have been proposed and widely adopted in the literature. These indices can be broadly categorized into classical performance indices and hybrid objective functions.

3.1. Classical Performance Indices

Classical performance indices are derived from the error signal

$$e(t) = V_{ref}(t) - V_t(t), \tag{4}$$

where $V_{\text{ref}}(t)$ denotes the reference voltage and $V_t(t)$ represents the terminal voltage of the generator.

These indices evaluate control performance by integrating different functions of the error signal over time. The IAE is defined as:

$$J_{IAE} = \int_0^T |e(t)| dt \tag{5}$$

The ISE is expressed as

$$J_{ISE} = \int_0^T e^2(t) dt \tag{6}$$

The ITAE is given by

$$J_{ITAE} = \int_0^T t |e(t)| dt \tag{7}$$

The ITSE is formulated as

$$J_{ITSE} = \int_0^T t e^2(t) dt \tag{8}$$

Although classical indices have been successfully applied in numerous AVR studies, their primary limitation lies in their exclusive focus on voltage tracking performance. None of these indices explicitly accounts for the magnitude or energy of the control signal, which becomes increasingly important in modern power systems under sustainability and efficiency constraints.

3.2. Hybrid Objective Functions

Hybrid objective functions combine multiple transient response metrics.

The ZLG index balances overshoot and response speed:

$$J_{ZLG} = \left(1 - e^{-\beta}\right) \cdot \left(M_p + E_{ss}\right) + e^{-\beta}\left(t_s - t_r\right) \tag{9}$$

where,

M_p denotes the maximum overshoot,
E_{ss} is the steady-state error,
t_s represents the settling time,
t_r is the rising time,
β is a weighting parameter that regulates the relative emphasis between transient magnitude and response speed.

This formulation allows the ZLG index to flexibly balance fast response and low overshoot by adjusting the parameter β. Despite its effectiveness in shaping transient behavior, the ZLG function does not explicitly incorporate control effort or control signal energy into the optimization process.

Another hybrid objective function considered in this study is the TR-based performance index, primarily designed to enhance transient response while improving robustness against parameter variations and external disturbances. Unlike classical indices, the TR objective function explicitly incorporates time-domain response measures and penalizes unfavorable transient behavior.

The TR objective function is defined as:

$$J_{TR} = \begin{cases} t_r + t_s + \delta\left(ISE + ITAE\right), & if \quad \%Mp > 0.1 \\ t_r + t_s + \left(ISE + ITAE\right), & otherwise \end{cases} \tag{10}$$

where,

t_r is the rise time,
t_s is the settling time,
δ is a weighting coefficient that panelizes parameter combinations leading to excessive overshoot,
$\%M_p$ denotes the percentage overshoot,
ISE is the Integral of Squared Error,
$ITAE$ is the Integral of Time-weighted Absolute Error.

This formulation enables the TR objective function to dynamically distinguish between acceptable and excessive overshoot. When the overshoot exceeds a predefined threshold, the penalty term weighted by λ is activated, effectively discouraging solutions with poor transient behavior. As a result, the TR index promotes fast and well-damped voltage responses while maintaining robustness under varying operating conditions.

4. PROPOSED ENERGY-EFFICIENT PERFORMANCE INDEX

Conventional and hybrid objective functions used in AVR controller optimization primarily focus on voltage-tracking performance and transient response. While such indices are effective in improving the rising time, settling time, and overshoot, they do not explicitly account for the energy associated with the control action. In modern power systems, where sustainability, efficiency, and hardware limitations are increasingly critical, neglecting control energy may lead to excessive actuator effort, unnecessary power consumption, and reduced long-term reliability.

To address this limitation, this study proposes a novel EEPI that explicitly integrates control signal energy into the optimization objective, while preserving desirable transient response characteristics. The proposed index is designed to establish a physically meaningful trade-off between voltage regulation quality and control effort.

4.1. Energy-Based Control Function Index

The control energy component is quantified through an ECFI, defined as the time integral of weighted control-signal related terms. The ECFI captures not only the magnitude of the control signal but also its dynamic variations, which are closely related to switching activity and energy expenditure in practical AVR implementations.

The ECFI is formulated as:

$$ECFI = \int_0^T \left(\omega_1 e^2(t) + \omega_2 u^2(t) + \omega_3 \left(\frac{du(t)}{dt} \right)^2 \right) dt \qquad (11)$$

where $u(t)$ denotes the controller output signal, and w_1, w_2, w_3 are weighting coefficients that balance voltage tracking accuracy, control magnitude, and control signal variation, respectively.

The weighting coefficients w_1, w_2, w_3 were selected based on the relative importance assigned to voltage tracking accuracy, control signal magnitude, and control signal variation within the proposed energy-aware control framework. In practical AVR operation, accurate voltage tracking and suppression of excessive control magnitude were prioritized, as these directly influence voltage regulation quality and actuator effort. Therefore, the coefficients associated with voltage tracking and control magnitude were assigned higher values, while the coefficient related to control signal variation was assigned a comparatively lower value to provide secondary penalization of rapid control fluctuations. This priority-based selection ensures that the optimization process primarily preserves voltage regulation performance while limiting unnecessary control effort. Preliminary simulations further confirmed that the selected coefficient set maintains voltage regulation accuracy while effectively suppressing excessive control activity. The selected numerical values and their physical interpretation are summarized in Table 3.

Table 3. EEPI and ECFI parameter settings used in this study

Parameter	Description	Selected value	Selection rationale
ω_1	Voltage tracking error weight	1	Prioritizes voltage tracking accuracy
ω_2	Control signal magnitude weight	1	Limits excessive control effort
ω_3	Control signal variation weight	0.5	Moderately penalizes control signal variation
α	Energy contribution coefficient	4.0	Balances energy suppression with transient response
γ	ECFI scaling coefficient	1.0	Normalizes ECFI contribution
β	Transient shaping parameter	1.0	Ensures consistent transient performance weighting
κ	Steady-state error penalty coefficient	100	Enforces strict steady-state accuracy
ε	Steady-state error threshold	0.002	Enforces strict voltage regulation accuracy

This formulation ensures that aggressive control actions with large amplitudes or rapid variations are penalized, directly reflecting their associated energy cost.

4.2. EEPI Cost Function Formulation

Building upon the ECFI definition, the proposed EEPI combines classical transient response indicators with the energy-based control effort term. The EEPI cost function is defined as:

$$J_{EEPI} = \begin{cases} \kappa\left[e^{-\beta} M_p + \left(1 - e^{-\beta}\right) \cdot \left(\alpha \cdot (t_s + t_r) + \gamma ECFI \right) \right], & |E_{ss}| > \varepsilon \\ e^{-\beta} M_p + \left(1 - e^{-\beta}\right) \cdot \left(\alpha \cdot (t_s + t_r) + \gamma ECFI \right) & otherwise \end{cases} \qquad (12)$$

where,

M_p denotes the maximum overshoot,
t_s and t_r represent the settling and rise times, respectively,
E_{ss} is the steady-state error,
ε is a predefined steady-state error threshold,
β is a shaping parameter controlling the relative emphasis between overshoot and energy-aware terms,
α, γ, and κ are positive weighting coefficients.

The EEPI parameters α, γ and κ, as well as the steady-state error threshold ε, were determined through a structured design-oriented tuning process aimed at achieving a balanced compromise between transient performance, energy suppression, and steady-state accuracy. The coefficient α was selected to regulate the relative contribution of the energy-related term within the EEPI, ensuring that energy minimization does not dominate transient response characteristics. The scaling parameter γ was introduced to maintain a consistent contribution of the ECFI term across different operating conditions. The penalty coefficient κ was assigned a sufficiently large value to strictly penalize infeasible steady-state behavior and enforce acceptable voltage regulation limits.

To ensure fair and reproducible comparison among different objective functions and controller structures, these parameter values were fixed and consistently used throughout all optimization runs. The final parameter set reflects a practical engineering compromise between control performance, energy efficiency, and steady-state accuracy. The selected values and their rationale are summarized in Table III.

The exponential weighting structure enables a smooth transition between transient-dominant and energy-dominant optimization behavior. Moreover, the conditional penalty applied when the steady-state error exceeds the specified threshold ensures strict voltage regulation accuracy.

In this study, the shaping parameter β is fixed to unity to ensure a balanced contribution of transient and energy-related terms. The steady-state error threshold ε is set to 0.002 to enforce strict voltage regulation accuracy.

5. PSO-BASED OPTIMIZATION FRAMEWORK

The tuning of AVR controller parameters constitutes a nonlinear, multi-parameter optimization problem characterized by strong coupling between transient performance and control effort. Analytical tuning approaches become ineffective under such conditions, particularly when nonlinear elements such as limiters and real-time execution constraints are considered. Therefore, a population-based metaheuristic optimization strategy is adopted to efficiently explore the solution space and identify near-global optimal parameter sets.

The PSO algorithm is selected in this study due to its fast convergence characteristics, low computational complexity, and strong performance reported in AVR controller tuning problems compared to other metaheuristic algorithms such as GWO and DE.

The optimization task aims to determine the optimal controller parameter vector that minimizes the proposed EEPI. Accordingly, the optimization problem is formulated as

$$\min \quad J_{EEPI}(\theta) \tag{13}$$

subject to

$$\theta_{\min} \leq \theta \leq \theta_{\max} \tag{14}$$

where θ denotes the controller parameter vector.

For the PID controller, the decision vector is defined as

$$\theta_{\mathrm{PID}} = [K_p, K_i, K_d] \tag{15}$$

whereas for the FOPID controller, it is given by

$$\theta_{\mathrm{FOPID}} = [K_p, K_i, K_d, \lambda, \mu] \tag{16}$$

The lower and upper bounds of each controller parameter are selected based on practical AVR operating constraints and commonly adopted ranges reported in the literature. These bounds define the feasible search space explored by the PSO algorithm and ensure physically meaningful controller configurations.

The search space boundaries used for the optimization of PID and FOPID controllers are summarized in Table 4.

Table 4. Boundaries for controller parameters

Controller	Parameter	Lower bound	Upper bound
PID	K_p	0.01	10
	K_i	0.001	1
	K_d	0.001	1
FOPID	K_p	0.01	10
	K_i	0.001	1
	K_d	0.001	1
	λ	0.1	1.5
	μ	0.05	1.2

Within the PSO algorithm, each particle represents a candidate controller parameter set and moves through the search space by updating its velocity and position according to

$$v_i^{k+1} = \omega v_i^k + c_1 r_1 \left(p_i - x_i^k\right) + c_2 r_2 \left(g - x_i^k\right) \tag{17}$$

$$x_i^{k+1} = x_i^k + v_i^{k+1} \tag{18}$$

where ω is the inertia weight, c1 and c2 denote the cognitive and social acceleration coefficients, respectively, and r1 and r2 are uniformly distributed random numbers in the interval [0,1]. The inertia weight is linearly decreased during the optimization process to ensure an effective balance between global exploration and local exploitation.

The optimization procedure is executed offline. For each particle, the EEPI value is evaluated by simulating the AVR system under the corresponding controller parameters, and the resulting fitness value guides the swarm evolution. The PSO configuration parameters, including swarm size, maximum iteration number, inertia weight limits, and acceleration coefficients, are listed in Table 5.

Although the optimization process is performed offline, the resulting optimal controller parameters are subsequently implemented and evaluated within a PIL environment using a TMS320F28035 control card. The PIL implementation setup employed in this study is illustrated in Figure 2.

Table 5. PSO Algorithm Parameters

Parameter	**Value**
Swarm size	30
Maximum iterations	500
Inertia weight	0.729
Cognitive coefficient	1.49445
Social coefficient	1.49445

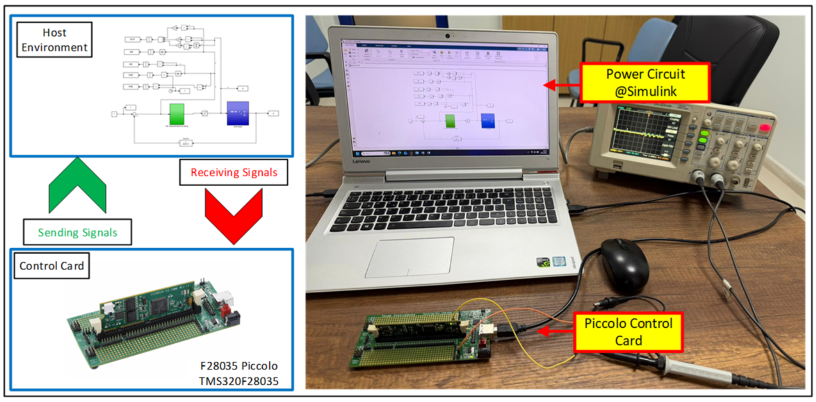

Figure 2. Processor-in-the-Loop (PIL) setup for real-time execution of the optimized AVR controllers on the TMS320F28035 control board

The real-time implementation is executed on a TMS320F28035 digital signal controller with a fixed sampling time of 1e-6 seconds. The optimized controller parameters obtained offline are embedded into the DSP, and the AVR model is executed in a PIL configuration, enabling cycle-accurate validation of the control performance under real-time constraints. The setup enables real-time execution of the optimized controllers while maintaining a seamless interface with the simulation environment.

6. RESULTS AND DISCUSSION

This section presents the performance evaluation of the AVR system using PID and FOPID controllers optimized under different objective functions. The proposed Energy-Efficient Performance Index (EEPI) is compared against classical performance indices (IAE, ISE, ITAE, ITSE) as well as hybrid objective functions (ZLG and TR). All optimization results are obtained using the same PSO configuration to ensure a fair and consistent comparison.

The optimized controller parameters obtained for each objective function are summarized in Table 6. These parameters are subsequently implemented in the AVR system, and all performance metrics reported in this section are evaluated based on the corresponding optimized controller settings executed within the Processor-in-the-Loop (PIL) environment using the TMS320F28035 control board.

Table 6. Optimized PID and FOPID controller parameters obtained using different objective functions

Optimized PID controller parameters according to different objective functions							
	Objective function						
	IAE	ISE	ITAE	ITSE	TR	ZLG	Proposed EEPI
K_p	1.7848	5.4040	5.2274	5.4127	4.4842	4.4288	0.6922
K_i	0.2910	0.3291	0.2897	0.3049	0.2708	0.2950	0.2289
K_d	0.3813	1.0000	1.0000	1.0000	0.9986	1.0000	0.1692
Optimized FOPID controller parameters according to different objective functions							
	Objective function						
	IAE	ISE	ITAE	ITSE	TR	ZLG	Proposed EEPI
K_p	5.6896	2.6241	5.6796	4.6171	5.1887	1.3589	0.9975
K_i	0.2832	0.4454	0.2803	1.0000	0.2064	0.3087	0.2711
K_d	1.0000	0.5454	1.0000	1.0000	1.0000	0.3123	0.2315
λ	1.0173	0.7694	1.0203	0.4456	1.1749	0.9757	1.0000
μ	1.0320	1.0078	1.0343	1.0094	1.0312	0.9956	1.0000

It is observed that some optimized controller parameters approach the upper bounds of the predefined search space. This behavior indicates that the optimization process tends to push the controller gains toward more aggressive configurations in order to improve transient response characteristics. However, the inclusion of the proposed EEPI formulation limits excessive parameter growth by penalizing high control energy, thereby resulting in more balanced and practically feasible controller parameter sets.

6.1. Transient Response Analysis

The transient responses of the AVR system obtained using PID and FOPID controllers optimized with different objective functions are illustrated in Fig. 3 and Fig. 4, respectively, while the corresponding time-domain performance metrics are summarized in Table 7 and Table 8 for the PID and FOPID controllers, respectively.

Table 7. Time-domain performance metrics of the AVR system using PID controllers optimized with different objective functions

Objective function	Rise time (s)	Overshoot (%)	Settling time 2% (s)	Settling time 5% (s)
IAE	0.3405	1.4134	1.0780	0.5360
ISE	0.3319	2.7102	1.0290	0.8350
ITAE	0.3314	1.6989	0.8800	0.8290
ITSE	0.3315	2.7553	1.0280	0.8350
TR	0.3693	0.0998	0.8760	0.8140
ZLG	0.5605	0.0977	0.8790	0.8140
Proposed EEPI	0.5155	0.9984	0.8480	0.7780

Table 8. Time-domain performance metrics of the AVR system using FOPID controllers optimized with different objective functions

Objective function	Rise time (s)	Overshoot (%)	Settling time 2% (s)	Settling time 5% (s)
IAE	0.3313	2.0169	0.9820	0.7880
ISE	0.3305	2.8702	1.2630	0.5170
ITAE	0.3314	1.9254	0.8520	0.7850
ITSE	0.3294	4.3828	1.4720	0.5120
TR	0.3421	0.1000	0.8520	0.7960
ZLG	0.3589	0.5121	0.6060	0.5630
Proposed EEPI	0.4096	1.0000	0.6760	0.6260

For the PID controller, classical performance indices such as IAE and ISE provide relatively fast initial responses but are associated with higher overshoot levels and less favorable damping characteristics. The ITAE and ITSE indices improve damping by penalizing sustained errors, resulting in smoother responses with comparable rise times. Hybrid objective functions, namely TR and ZLG, achieve very low overshoot by explicitly penalizing transient magnitude, although this often comes at the expense of slightly slower dynamic response.

The PID controller optimized using the proposed EEPI exhibits a moderately slower rise time compared to classical indices, reflecting the inherent trade-off between response speed and energy efficiency. However, the settling time remains competitive, and the response maintains stable and well-damped characteristics. This behavior indicates that the EEPI does not prioritize aggressive transient speed but instead selects a balanced operating point where acceptable dynamic performance is achieved alongside reduced control effort.

A similar trend is observed for the FOPID controller. Due to the additional tuning flexibility provided by fractional-order parameters, the FOPID structure generally achieves improved damping and faster settling compared to PID across most objective functions. The EEPI-optimized FOPID controller exhibits a slightly slower rise time compared to purely transient-oriented indices, yet maintains competitive settling performance and stable voltage regulation. These results confirm that the EEPI preserves acceptable transient behavior while enabling energy-aware optimization.

Overall, the transient analysis highlights a fundamental multi-objective trade-off between response speed and control energy. While classical and hybrid indices primarily target aggressive transient performance, the proposed EEPI intentionally moderates the control action to achieve a balanced compromise between dynamic response and energy efficiency.

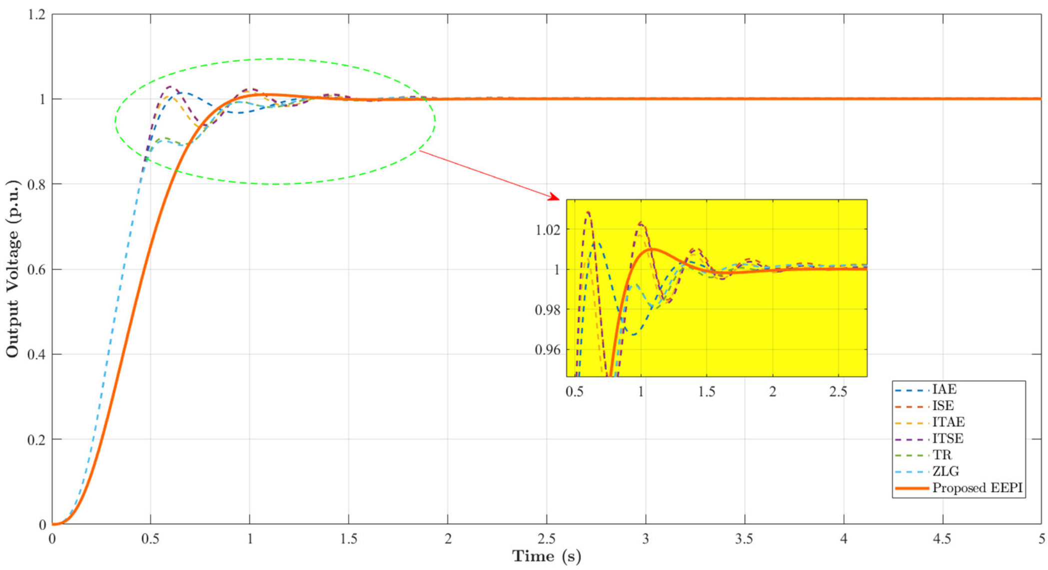

Figure 3. Transient response characteristics of the AVR system using PID controllers optimized with different objective functions

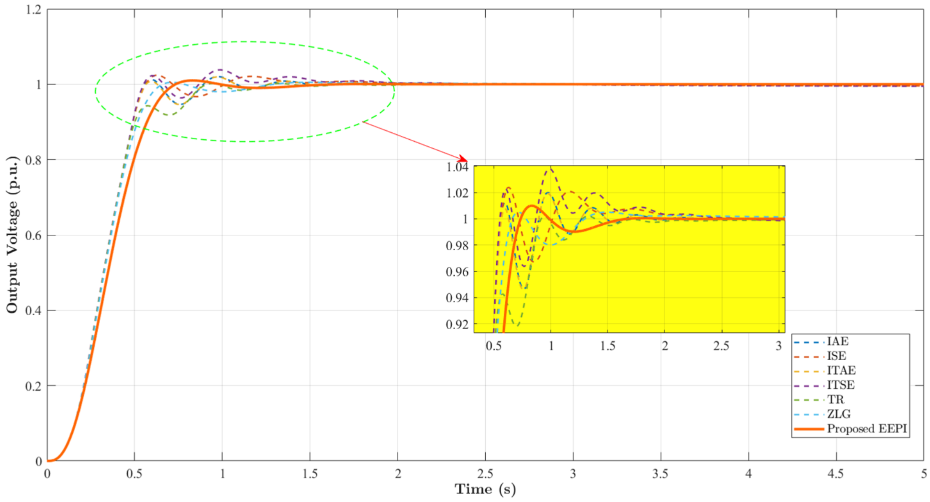

Figure 4. Transient response characteristics of the AVR system using FOPID controllers optimized with different objective functions

6.2. Control Effort and Energy Consumption

Beyond transient response characteristics, the control effort associated with each optimization strategy is examined to assess the practical efficiency of the AVR controllers. The corresponding control signals and cumulative control energy profiles obtained during PIL execution are illustrated in Fig.5, Fig.6 for the PID controller and Fig.7, Fig.8 for the FOPID controller.

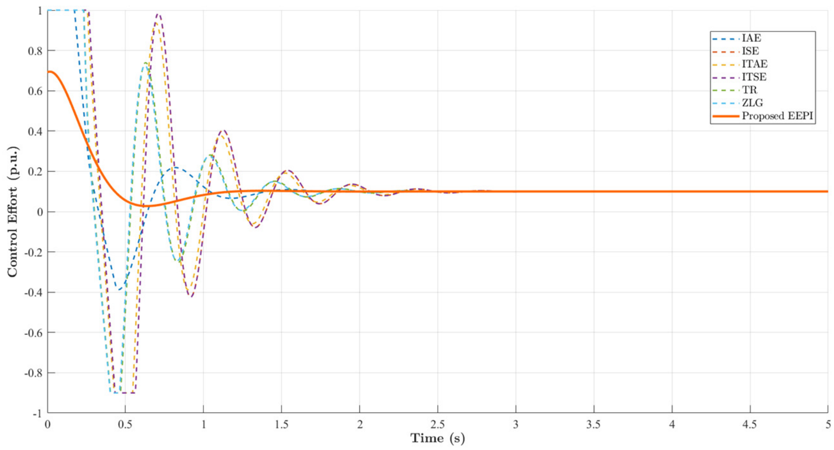

Figure 5. Control signal of the PID controller optimized using different objective functions

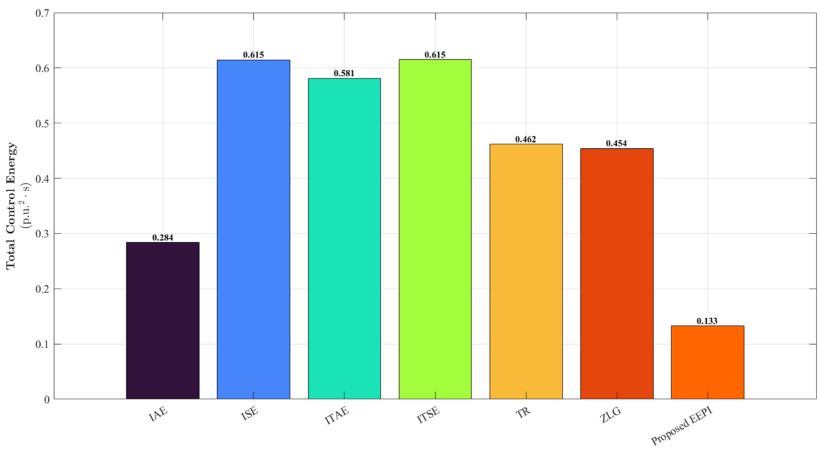

Figure 6. Total control energy comparison of the PID controller for different objective functions

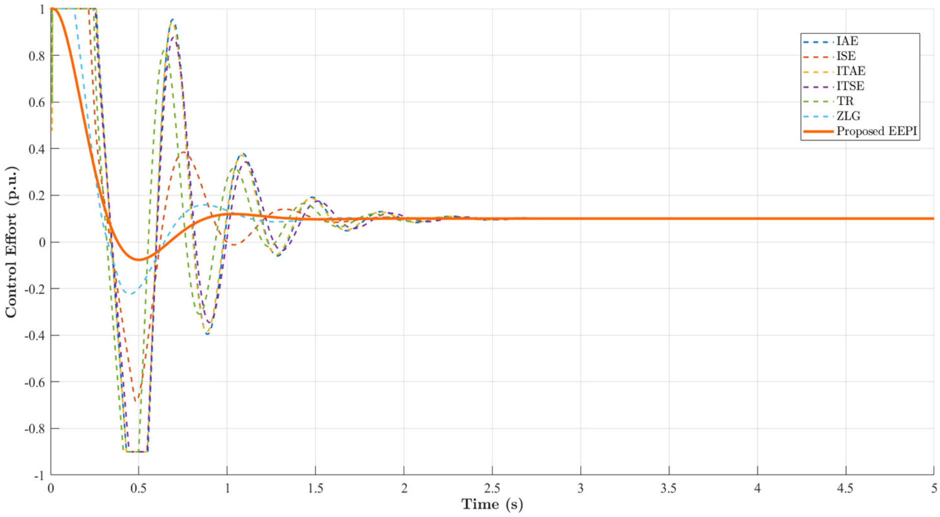

Figure 7. Control signal of the FOPID controller optimized using different objective functions

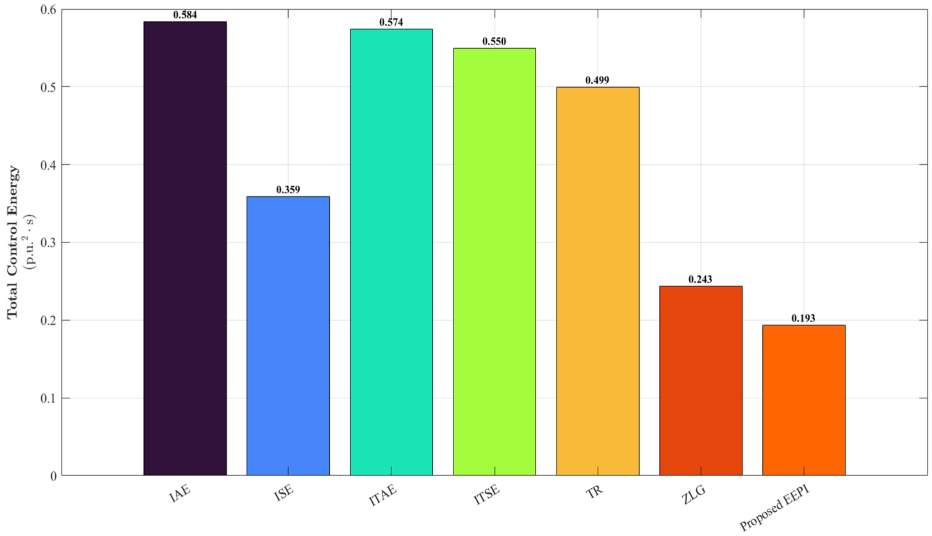

Figure 8. Total control energy comparison of the FOPID controller for different objective functions

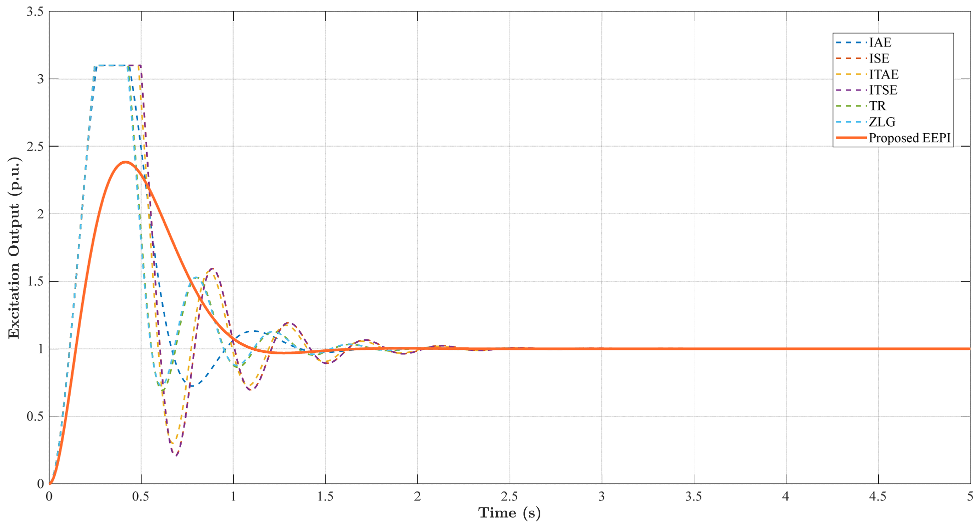

Figure 9. Excitation output of the PID controller optimized using different objective functions

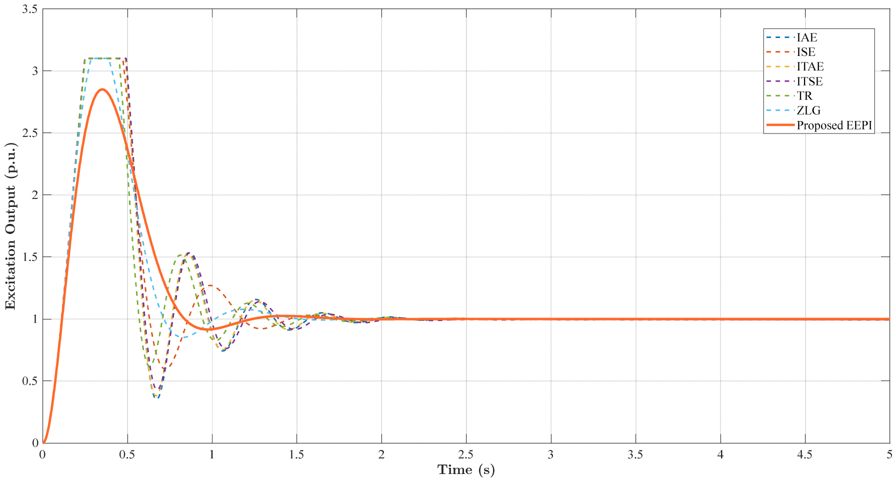

Figure 10. Excitation output of the FOPID controller optimized using different objective functions

For controllers optimized using classical objective functions, such as IAE, ISE, ITAE, and ITSE, the control signals exhibit pronounced oscillatory behavior with relatively high peak amplitudes during the transient period. These oscillations indicate frequent and abrupt control actions, which are directly associated with increased switching activity in the excitation system as clearly seen from the Fig. 9 and Fig. 10. In practical AVR implementations, such behavior leads to elevated switching losses and increased thermal stress on power electronic components.

Hybrid objective functions, namely ZLG and TR, partially mitigate this effect by improving damping characteristics; however, noticeable oscillations and relatively large control excursions are still observed, particularly during the early transient interval. Although these strategies improve voltage response smoothness compared to classical indices, the resulting control effort remains non-negligible.

In contrast, the proposed EEPI achieves a markedly lower cumulative control energy for the PID controller, with a value of 0.1329, corresponding to a reduction of approximately 70.7% relative to the best-performing hybrid objective function (ZLG: 0.4541) and 71.2% relative to the TR-based formulation (0.4618). This substantial reduction indicates that the EEPI effectively suppresses excessive control oscillations while maintaining favorable transient response characteristics.

Similar trends are observed for the FOPID controller. Owing to the additional tuning flexibility provided by the fractional-order parameters, the FOPID structure generally yields improved control smoothness compared to its PID counterpart. The EEPI-optimized FOPID controller achieves a cumulative control energy of 0.1933, which represents a reduction of approximately 20.5% compared to the ZLG-based solution (0.2432) and 61.3% compared to the TR-based objective function (0.4992).

Overall, these results confirm that excessive control oscillations significantly increase control energy consumption and switching losses in AVR systems. By explicitly incorporating control energy into the optimization objective, the proposed EEPI enables a substantial reduction in control effort for both PID and FOPID controllers, resulting in improved energy efficiency, reduced actuator stress, and enhanced practical viability under realistic execution conditions.

7. CONCLUSIONS

This study presented a novel energy-efficient optimization framework for AVR controllers based on a newly developed EEPI. Unlike classical and hybrid objective functions that primarily emphasize aggressive transient performance, the proposed EEPI explicitly incorporates control signal energy into the optimization process, enabling a balanced compromise between voltage regulation performance and control effort.

The proposed framework was applied to both PID and FOPID controllers, with controller parameters optimized using the PSO algorithm under identical configuration settings to ensure fair and consistent comparison. The comparative analysis revealed that, although the EEPI may produce slightly slower rise times compared to purely transient-oriented indices, it preserves competitive settling behavior and stable voltage regulation while significantly reducing control effort. This confirms the inherent trade-off between response speed and energy efficiency and demonstrates that the EEPI converges to a balanced operating point rather than prioritizing aggressive transient response.

Beyond transient characteristics, the EEPI achieved a substantial reduction in cumulative control energy and control signal oscillations for both PID and FOPID controllers. The resulting smoother control behavior reduces switching activity, actuator stress, and associated energy losses in practical AVR implementations. These improvements contribute to enhanced energy efficiency, improved hardware reliability, and reduced long-term operational stress without compromising voltage regulation quality.

The implementation of the optimized controllers within a PIL environment using a TMS320F28035 control platform further verified the practical feasibility of the proposed approach. The close agreement between simulation and real-time execution results confirms that the EEPI-based framework is suitable for realistic AVR applications where energy efficiency, actuator limitations, and implementation constraints must be considered simultaneously.

Overall, the proposed EEPI provides a systematic and scalable methodology for energy-aware AVR controller tuning. By explicitly incorporating control energy into the optimization objective, the framework introduces an energy-conscious perspective to AVR design and contributes toward sustainable and efficient voltage regulation in modern power systems. Future work may extend the proposed framework to multi-machine power systems to investigate inter-machine dynamic interactions and potential resonance phenomena, as well as to adaptive excitation systems and real-time optimization under varying operating conditions.

8. REFERENCES

1. Gopi, P., Reddy, S.V., Bajaj, M., Zaitsev, I. & Prokop, L. (2024). Performance and robustness analysis of V-Tiger PID controller for automatic voltage regulator. *Scientific Reports, 14*(1), 7867.
2. Teke, A., Sarıbulut, L. & Tümay, M. (2011). Power quality disturbances and custom power devices. *Çukurova Üniversitesi Mühendislik-Mimarlık Fakültesi Dergisi, 26*(1), 57-65.
3. Tekin, P. (2022). Çukurova bölgesi için kısa vadeli yapay zeka tabanlı rüzgar güç tahmini. *Çukurova Üniversitesi Mühendislik Fakültesi Dergisi, 37*(4), 1143-1154.
4. Micev, M., Ćalasan, M. & Radulović, M. (2023). Optimal tuning of the novel voltage regulation controller considering the real model of the automatic voltage regulation system. *Heliyon, 9*(8), e18707.
5. Chatterjee, S. & Mukherjee, V. (2016). PID controller for automatic voltage regulator using teaching–learning based optimization technique. *International Journal of Electrical Power & Energy Systems, 77*, 418-429.
6. Pan, I. & Das, S. (2012). Chaotic multi-objective optimization based design of fractional order PIλDμ controller in AVR system. *International Journal of Electrical Power & Energy Systems, 43*(1), 393-407.
7. Veinović, S., Stojić, D. & Joksimović, D. (2022). Optimized four-parameter PID controller for AVR systems with respect to robustness. *International Journal of Electrical Power & Energy Systems, 135*, 107529.
8. Gaing, Z.-L. (2004). A particle swarm optimization approach for optimum design of PID controller in AVR system. *IEEE Transactions on Energy Conversion, 19*(2), 384-391.
9. Dogruer, T. & Can, M.S. (2022). Design and robustness analysis of fuzzy PID controller for automatic voltage regulator system using genetic algorithm. *Transactions of the Institute of Measurement and Control, 44*(9), 1862-1873.
10. Gozde, H. & Taplamacioglu, M.C. (2011). Comparative performance analysis of artificial bee colony algorithm for automatic voltage regulator (AVR) system. *Journal of the Franklin Institute, 348*(8), 1927-1946.
11. Kar, M.K., Kumar, S., Singh, A.K., Panigrahi, S. & Cherukuri, M. (2022). Design and analysis of FOPID-based damping controllers using a modified Grey Wolf Optimization algorithm. *International Transactions on Electrical Energy Systems, 2022*, 1-31.
12. Bingul, Z. & Karahan, O. (2018). A novel performance criterion approach to optimum design of PID controller using cuckoo search algorithm for AVR system. *Journal of the Franklin Institute, 355*(13), 5534-5559.

13. Sahin, A.K., Cavdar, B. & Ayas, M.S. (2024). An adaptive fractional controller design for automatic voltage regulator system: sigmoid-based fractional-order PID controller. *Neural Computing and Applications, 36*(23), 14409-14431.

14. Veinović, S., Stojić, D. & Ivanović, L. (2023). Optimized PIDD2 controller for AVR systems regarding robustness. *International Journal of Electrical Power & Energy Systems, 145*, 108646.

15. Panda, S., Sahu, B.K. & Mohanty, P.K. (2012). Design and performance analysis of PID controller for an automatic voltage regulator system using simplified particle swarm optimization. *Journal of the Franklin Institute, 349*(8), 2609-2625.

16. Mohanty, P.K., Sahu, B.K. & Panda, S. (2014). Tuning and assessment of proportional–integral–derivative controller for an automatic voltage regulator system employing local unimodal sampling algorithm. *Electric Power Components and Systems, 42*(9), 959-969.

17. Duman, S., Yörükeren, N. & Altaş, İ.H. (2016). Gravitational search algorithm for determining controller parameters in an automatic voltage regulator system. *Turkish Journal of Electrical Engineering & Computer Sciences, 24*, 2387-2400.

18. Shouran, M. & Alenezi, M. (2025). A novel fuzzy PIDF enhancing PIDF controller tuned in two stages by TLBO and PSO algorithms for reliable AVR performance. *IEEE Access, 13*, 93505-93522.

19. Sekyere, Y.O.M., Ajiboye, P.O., Effah, F.B. & Opoku, B.T. (2025). Optimizing PID control for automatic voltage regulators using ADIWACO PSO. *Scientific African, 27*, e02562.

20. Eltag, K., Abdullahi, S., Weining, L. & Xiaohu, C. (2025). Design TLBO fuzzy fractional order PID filter controller for AVR excitation system. *IEEE Access, 13*, 216466-216495.

21. Izci, D., Abualigah, L., Can, Ö., Andiç, C. & Ekinci, S. (2025). A novel cascaded RPIDD²-PI controller tuned by enhanced cooperation search algorithm for automatic voltage regulator systems. *IET Control Theory & Applications, 19*(1).

22. Chetty, N.D., Sharma, G., Gandhi, R. & Çelik, E. (2024). A novel salp swarm optimization oriented 3-DOF-PIDA controller design for automatic voltage regulator system. *IEEE Access, 12*, 20181-20196.

23. Dai, F. & Gao, S. (2024). Optimal design of a PIDD² controller for an AVR system using hybrid whale optimization algorithm. *IEEE Access, 12*, 128525-128540.

24. Türksoy, Ö. & Türksoy, A. (2024). A fast and robust sliding mode controller for automatic voltage regulators in electrical power systems. *Engineering Science and Technology, an International Journal, 53*, 101697.

25. Izci, D., Ekinci, S. & Zeynelgil, H.L. (2024). Controlling an automatic voltage regulator using a novel Harris hawks and simulated annealing optimization technique. *Advanced Control for Applications, 6*(2), 1-26.

26. Izci, D., Abualigah, L., Can, Ö., Andiç, C. & Ekinci, S. (2024). Achieving improved stability for automatic voltage regulation with fractional-order PID plus double-derivative controller and mountain gazelle optimizer. *International Journal of Dynamics and Control, 12*(7), 2550-2565.

27. Ahmadnia, M., Hajipour, A. & Tavakoli, H. (2024). Robust variable-order fractional PID-LP fuzzy controller for automatic voltage regulator systems. *Applied Soft Computing, 167*, 112268.

28. Saka, M. (2024). Novel hVsaGwo algorithm for non-linear dynamic weighted state feedback with 1DOF-PID based controllers in AVR. *Engineering Science and Technology, an International Journal, 59*, 101857.

29. Furat, M. & Cucu, G.G. (2022). Design, implementation, and optimization of sliding mode controller for automatic voltage regulator system. *IEEE Access, 10*, 55650-55674.

30. Micev, M., Ćalasan, M., Ali, Z.M., Hasanien, H.M. & Abdel Aleem, S.H.E. (2021). Optimal design of automatic voltage regulation controller using hybrid simulated annealing–manta ray foraging optimization algorithm. *Ain Shams Engineering Journal, 12*(1), 641-657.

31. Micev, M., Ćalasan, M. & Oliva, D. (2021). Design and robustness analysis of an automatic voltage regulator system controller by using equilibrium optimizer algorithm. *Computers & Electrical Engineering, 89*, 106930.

32. Eke, I., Saka, M., Gozde, H., Arya, Y. & Taplamacioglu, M.C. (2021). Heuristic optimization based dynamic weighted state feedback approach for 2DOF PI-controller in automatic voltage regulator. *Engineering Science and Technology, an International Journal, 24*(4), 899-910.

33. Kose, E. (2020). Optimal control of AVR system with tree seed algorithm-based PID controller. *IEEE Access, 8*, 89457-89467.

34. Jumani, T.A., Mustafa, M.W., Rasid, M.M., Saeed, M.S. Khan, İ. & Nisar, K.S. (2020). Jaya optimization algorithm for transient response and stability enhancement of a fractional-order PID based automatic voltage regulator system. *Alexandria Engineering Journal, 59*(4), 2429-2440.

35. Ekinci, S. & Hekimoglu, B. (2019). Improved kidney-inspired algorithm approach for tuning of PID controller in AVR system. *IEEE Access, 7*, 39935-39947.

36. Zhou, Y., Zhang, J., Yang, X. & Ling, Y. (2019). Optimization of PID controller based on water wave optimization for an automatic voltage regulator system. *Information Technology and Control, 48*(1).

37. Çelik, E. (2018). Incorporation of stochastic fractal search algorithm into efficient design of PID controller for an automatic voltage regulator system. *Neural Computing and Applications, 30*(6), 1991-2002.

38. Furat, M. (2023). Chattering attenuation analysis in variable structure control for automatic voltage regulator with input constraints. *Engineering Science and Technology, an International Journal, 45*, 101499.

39. IEEE (2006). IEEE recommended practice for excitation system models for power system stability studies. *IEEE Power Engineering Society,* 95.

9. NOMENCLATURE

ABC	Artificial Bee Colony	ITSE	Integral of Time-weighted Squared Error
AVR	Automatic Voltage Regulator	JOA	Jaya Optimization Algorithm
CSA	Cuckoo Search Algorithm	MGO	Mountain Gazelle Optimizer
DE	Differential Evolution	MRFO	Manta Ray Foraging Optimization
ECFI	Energy-Based Control Function Index	PID	Proportional–Integral–Derivative
ECSA	Enhanced Crow Search Algorithm	PIL	Processor-in-the-Loop
EEPI	Energy-Efficient Performance Index	PSO	Particle Swarm Optimization
EO	Equilibrium Optimizer	SCA	Sine Cosine Algorithm
FOPID	Fractional-Order Proportional–Integral–Derivative	SFS	Stochastic Fractal Search
GA	Genetic Algorithm	SMC	Sliding Mode Control
GWO	Grey Wolf Optimization	SSO	Salp Swarm Optimization
HWO	Hybrid Whale Optimization	TLBO	Teaching-Learning-Based Optimization
IAE	Integral of Absolute Error	TR	Turksoy
IKA	Improved Kidney-Inspired Algorithm	TSA	Tree Seed Algorithm
ISE	Integral of Squared Error	WWO	Water Wave Optimization
ITAE	Integral of Time-weighted Absolute Error	ZLG	Zwe-Lee Gaing